

On the boundary element method for billiards with corners

This article has been downloaded from IOPscience. Please scroll down to see the full text article.

2005 J. Phys. A: Math. Gen. 38 6675

(<http://iopscience.iop.org/0305-4470/38/30/004>)

View [the table of contents for this issue](#), or go to the [journal homepage](#) for more

Download details:

IP Address: 171.66.16.92

The article was downloaded on 03/06/2010 at 03:51

Please note that [terms and conditions apply](#).

On the boundary element method for billiards with corners

Y Okada¹, A Shudo¹, S Tasaki² and T Harayama³

¹ Department of Physics, Tokyo Metropolitan University, 1-1 Minami-Ohsawa, Hachioji, Tokyo 192-0397, Japan

² Department of Applied Physics, Waseda University, 3-4-1 Okubo, Shinjuku-ku, Tokyo 169-8555, Japan

³ Department of Nonlinear Science, ATR Wave Engineering Laboratories, 2-2 Hikaridai, Seika-cho, Soraku-gun, Kyoto 619-02, Japan

Received 31 March 2005, in final form 15 June 2005

Published 13 July 2005

Online at stacks.iop.org/JPhysA/38/6675

Abstract

The boundary element method is one of the reliable numerical schemes to solve the eigenvalue problem of the Helmholtz equation, which is justified by the Fredholm theory for domains with a smooth boundary. When a domain has corners, however, the corresponding integral equation is singular, so that the boundary element method lacks its well-established base. Employing a cutoff technique, we here formulate a well-grounded version of the boundary element method, and also give a certain justification to the standard boundary element method even for domains with corners.

PACS number: 05.45.Mt

1. Introduction

The billiard system plays a central role in the study of quantum chaos [1]. This is because one can control underlying classical dynamics only by deforming the shape of the billiard tables. In particular, conjectured universalities of level statistics are often tested employing billiard systems such as the Sinai, stadium or dispersing billiards where full chaotic behaviour is shown to be realized [2]. Also, polygonal billiards recently attract much attention as intermediate systems standing between integrable and chaotic ones. It was numerically suggested that level statistics of polygonal billiards significantly deviates from the GOE universality class [3]. A semiclassical argument to understand such marginal systems has been developed [4] and the importance of diffractive corrections has been recognized [5–7]. The isospectral problems also concern the billiard system [8], and as far as planar billiards are concerned, all known isospectral examples have corners [9–13].

In any case, we often encounter and need to investigate billiard tables with cusps, corners or other types of non-smooth boundaries. A problem of corners can be recognized, for instance,

when one numerically obtains the quantum energy levels of a billiard system by using plane wave decomposition [14]. Though each eigenstate of a billiard, except for non-convex one [15], can be approximated by the superposition of real plane waves, it has been reported that a number of eigenstates are missed in a numerical procedure based on the real plane wave decomposition for domains with corners [16]. This puzzling situation originates from the fact that singular superposition is needed for the eigenstate of a billiard with corners; in other words, evanescent modes should be included in the basis to obtain the eigenstates, because of the presence of corners [16–18].

The boundary element method (BEM) is another numerical method to solve the eigenvalue problem of the Helmholtz equation. It has been applied to billiards with a wider class of geometries including non-convex ones [19–22]. However, also in the BEM, we inevitably encounter problems of singularity caused by the presence of corners [24]. As discussed in this paper, the BEM is based on a Fredholm integral equation of the second kind whose integral kernel is determined by the geometry of the billiard, and eigenenergies are obtained as real zeros of the discretized Fredholm determinant [25, 26]. When the billiard has corners, however, the integral kernel becomes singular. This means that the convergence of the determinant cannot be guaranteed only within the Fredholm theory. That is, the BEM lacks a well-established basis if the billiard has corners.

This paper is devoted to providing a well-grounded version of BEM for billiards with corners. In section 2, we will state problems caused by corners more explicitly. In section 3, we will derive a non-singular integral equation for billiards with corners, and also provide a certain justification for the standard BEM. Section 4 concludes and summarizes the paper.

2. Corner problem in the BEM

In this section, we formulate the BEM and specify our problem for billiards with corners. The equation considered here is the Schrödinger–Helmholtz equation for the domain Ω :

$$(\Delta + k^2)\Psi(\mathbf{r}) = 0, \quad \mathbf{r} \in \Omega, \quad (1)$$

with the homogeneous Dirichlet boundary condition

$$\Psi^-(\mathbf{r}) := \lim_{\Omega \ni \mathbf{r}' \rightarrow \mathbf{r}} \Psi(\mathbf{r}') = 0, \quad \mathbf{r} \in \partial\Omega, \quad (2)$$

where $k = \sqrt{2mE}/\hbar$. Hereafter the domain Ω is assumed to be enclosed with the boundary $\partial\Omega$ consisting of a finite number of C^2 arcs $\{\Gamma_1, \Gamma_2, \dots, \Gamma_m\}$ and a set of corner points $\{p_1, p_2, \dots, p_m\}$. The interior angle of each corner p_i , which is defined by the angle of intersecting tangent lines at the corner, is denoted by γ_i . A typical example is illustrated in figure 1.

In order to convert equations (1) and (2) into an integral equation, we express the solution of equation (1) with equation (2) as the double-layer potential with a density ρ :

$$\Psi(\mathbf{r}) = \int_{\partial\Omega} \frac{\partial G_0(\mathbf{r}, \mathbf{r}(s); k)}{\partial v_s} \rho(s) ds, \quad \mathbf{r} \in \Omega, \quad (3)$$

where v_s denotes the outer unit normal at the point $\mathbf{r}(s) \in \partial\Omega$ with an arc length parameter s and G_0 is the free Green's function defined as

$$G_0(\mathbf{r}, \mathbf{r}'; k) = -\frac{i}{4} H_0^{(1)}(k|\mathbf{r} - \mathbf{r}'|). \quad (4)$$

Here $H_0^{(1)}$ denotes the zero-order Hankel function of the first kind. The integral over $\partial\Omega$ should be read as the sum of improper integrals: $\int_{\Gamma_1} + \int_{\Gamma_2} + \dots + \int_{\Gamma_m}$, because v_s cannot be defined at the corners. The double-layer potential $\Psi(\mathbf{r})$ clearly satisfies the Helmholtz equation (1)

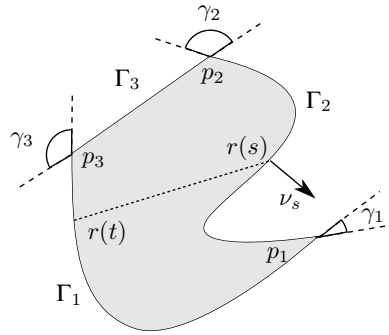


Figure 1. A domain with corners. The boundary consists of a finite number of C^2 arcs and corners.

at each interior point $r \in \Omega$, thus $\Psi(r)$ becomes a solution of the Dirichlet problem if the boundary condition (2) is fulfilled. Since the boundary value of the double-layer potential (3) can be written as

$$\Psi^-(r(t)) = \begin{cases} \int_{\partial\Omega} \frac{\partial G_0(r(t), r(s); k)}{\partial \nu_s} \rho(s) ds + \frac{1}{2} \rho(t), & r(t) \in \partial\Omega \setminus \{p_1, p_2, \dots, p_m\}, \\ \int_{\partial\Omega} \frac{\partial G_0(r(t), r(s); k)}{\partial \nu_s} \rho(s) ds + \frac{\gamma_i}{2\pi} \rho(t), & r(t) = p_i \in \{p_1, p_2, \dots, p_m\}, \end{cases} \tag{5}$$

we obtain an equivalent integral equation for the original problems (1) and (2),

$$\begin{cases} \rho(t) - \int_{\partial\Omega} K(t, s; k) \rho(s) ds = 0, & r(t) \in \partial\Omega \setminus \{p_1, p_2, \dots, p_m\}, \\ \frac{\gamma_i}{\pi} \rho(t) - \int_{\partial\Omega} K(t, s; k) \rho(s) ds = 0, & r(t) = p_i \in \{p_1, p_2, \dots, p_m\}, \end{cases} \tag{6}$$

where

$$\begin{aligned} K(t, s; k) &:= -2 \frac{\partial G_0(r(t), r(s); k)}{\partial \nu_s} \\ &= -\frac{ik}{2} \frac{[r(s) - r(t)] \cdot \nu_s}{|r(s) - r(t)|} H_1^{(1)}(k|r(s) - r(t)|). \end{aligned} \tag{7}$$

Here we note that the integral exists as an improper integral in equation (6), even if the diagonal of the integral kernel (7) cannot be defined.

Discretizing the boundary integral in equation (6) with appropriate quadrature points $\{s_1, s_2, \dots, s_n\}$ and their weights $\{w_1, w_2, \dots, w_n\}$, one can reduce the integral equation to a n -dimensional linear system:

$$\rho(s_i) - \sum_{j=1}^n w_j K(s_i, s_j; k) \rho(s_j) = 0. \tag{8}$$

Since the linear system (8) has a non-trivial solution if and only if

$$\Delta^{(n)}(k) := \det[\delta_{ij} - w_j K(s_i, s_j; k)] = 0, \tag{9}$$

where δ_{ij} denotes the Kronecker delta, each zero of $\Delta^{(n)}(k)$ is expected to approximate an eigenvalue of the original problems (1) and (2) when the number of quadrature points is sufficiently large. The required number of quadrature points n is determined by comparing

the de Broglie wavelength and the mean distance between the quadrature points. For given k , the corresponding de Broglie wavelength λ_k is given as $2\pi/k$, so we should take n sufficiently larger than $n_k = |\partial\Omega|k/2\pi$. We call the procedure giving approximate eigenvalues as the zeros of the determinant (9) the *standard BEM* in this paper.

Here we should refer to the transposed integral equation of (6), which is also used to formulate a BEM in the literature [19]. If we express a solution of (1) as a single-layer potential

$$\Psi(\mathbf{r}) = \int_{\partial\Omega} G_0(\mathbf{r}, \mathbf{r}(s); k) \mu(s) ds, \quad \mathbf{r} \in \Omega, \quad (10)$$

the transposed integral equation

$$\mu(t) - \int_{\partial\Omega} -2 \frac{\partial G_0(\mathbf{r}(t), \mathbf{r}(s); k)}{\partial \nu_t} \mu(s) ds = 0, \quad (11)$$

follows from the boundary condition (2) by the gap relation for the normal derivative of the single-layer potential. It is obvious that the corresponding determinant of the discretized integral equation coincides with (9) if quadrature points are chosen to avoid the corners at which the transposed integral equation (11) is not defined. So it is sufficient to concentrate on equation (6) in the following.

Now let us focus on the infinite-dimensional determinant $\lim_{n \rightarrow \infty} \Delta^{(n)}(k)$. To confirm that the standard BEM gives correct eigenvalues of the Dirichlet problems (1) and (2), it must be proved that the determinant (9) converges as $n \rightarrow \infty$ and its zeros coincide with the eigenvalues. As far as the domain enclosed with a single closed C^2 curve is concerned, this is guaranteed by the Fredholm theory for the integral equation defined by a continuous kernel. Since the behaviour of the Hankel function around $\tau(s, t) := |\mathbf{r}(s) - \mathbf{r}(t)| = 0$ is given as

$$H_1^{(1)}(k\tau(s, t)) = -\frac{2i}{\pi k\tau(s, t)} + \mathcal{O}(k\tau(s, t)(1 + \log k\tau(s, t))), \quad (12)$$

the diagonal of the integral kernel (7) is not defined by definition (7). However, we also have

$$\frac{[\mathbf{r}(s) - \mathbf{r}(t)] \cdot \nu_s}{|\mathbf{r}(s) - \mathbf{r}(t)|} = \frac{1}{2} \kappa(t) \tau(s, t) + \mathcal{O}(\tau(s, t)^2), \quad (13)$$

so the singularity of the Hankel function is compensated. The integral kernel K can thus be continuously extended onto the whole of $\partial\Omega \times \partial\Omega$ by putting the diagonal as

$$K(t, t; k) = -\frac{\kappa(t)}{2\pi}. \quad (14)$$

Here $\kappa(t)$ denotes the curvature of the boundary at the point $\mathbf{r}(t)$. Thus, one can apply the Fredholm theory to prove that the determinant (9) converges to the Fredholm determinant defined as

$$D(k) := 1 + \sum_{n=1}^{\infty} D_n(k), \quad (15)$$

where

$$D_n(k) := \frac{(-1)^n}{n!} \int_{\partial\Omega} ds_1 \cdots \int_{\partial\Omega} ds_n \begin{vmatrix} K(s_1, s_1; k) & \cdots & K(s_1, s_n; k) \\ \vdots & \ddots & \vdots \\ K(s_n, s_1; k) & \cdots & K(s_n, s_n; k) \end{vmatrix}, \quad (16)$$

and the integral equation (6) has a non-trivial solution if and only if $D(k) = 0$ [27].

When the domain has corners, in contrast, the infinite-dimensional determinant $\lim_{n \rightarrow \infty} \Delta^{(n)}(k)$ does not immediately make sense as it stands. In fact, the divergence in (12)

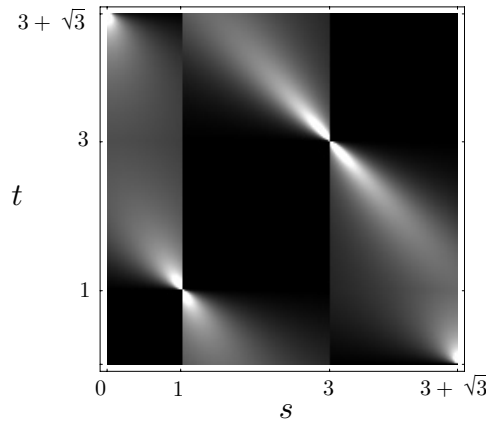


Figure 2. Density plot of $|K(t, s; k)|$ ($k = 21.5$) for the $\pi/2-\pi/3-\pi/6$ -angled triangular domain. The horizontal and vertical directions represent s and t , respectively, and brightness the absolute value of $K(t, s; k)$. The points $(0, 0)$, $(1, 1)$ and $(3, 3)$ correspond to corners with interior angles $\pi/2$, $\pi/3$ and $\pi/6$, respectively.

cannot be cancelled when $r(s)$ and $r(t)$ approach each other from opposite sides of a corner. Hence, the integral kernel (7) is not of Hilbert–Schmidt type and one cannot apply the Fredholm theory in order to guarantee that the standard BEM gives the correct eigenvalues for the domain with corners.

Here, we should mention a singular boundary integral equation derived for billiards subjected to a constant magnetic field [23]. However, the integral kernel discussed there has a singularity of type $1/\tau^2$, whereas our integral kernel (7) has a singularity of type $1/\tau$.

The singularity of the integral kernel (7) causes difficulties in numerical computation of the determinant (9) appearing in the standard BEM. Recalling that the integral appearing in equation (6) is an improper integral, we here numerically examine the determinant by introducing a cutoff kernel

$$K^{(\xi)}(t, s; k) := h_\xi(|t - s|)K(t, s; k), \tag{17}$$

where

$$h_\xi(x) := \begin{cases} 0, & |x| \leq \frac{\xi}{2}, \\ \frac{2}{\xi}x - 1, & \frac{\xi}{2} \leq |x| \leq \xi, \\ 1, & \xi \leq |x|. \end{cases} \tag{18}$$

Note that the determinant

$$\Delta^{(\xi, n)}(k) := \det[\delta_{ij} - w_j K^{(\xi)}(s_i, s_j; k)] \tag{19}$$

is guaranteed to converge to its Fredholm determinant, say $D^{(\xi)}(k)$, for each $\xi > 0$, because the kernel $K^{(\xi)}$ is bounded and piecewise continuous.

To see the nature of the determinant $\Delta^{(\xi, n)}(k)$, as an example, we here take the $\pi/2-\pi/3-\pi/6$ -angled triangle, whose eigenvalue spectrum is analytically known. The profile of its integral kernel is presented in figure 2. One can see that the integral kernel $K(t, s; k)$ diverges around the corners if s and t are located on the opposite sides of each corner. As depicted in figure 3, if one uses a cutoff kernel with a certain finite cutoff length ξ , $\Delta^{(\xi, n)}(k)$ certainly converges with the increase of n . However, figure 4 shows that $D^{(\xi)}(k)$ tends to zero as the

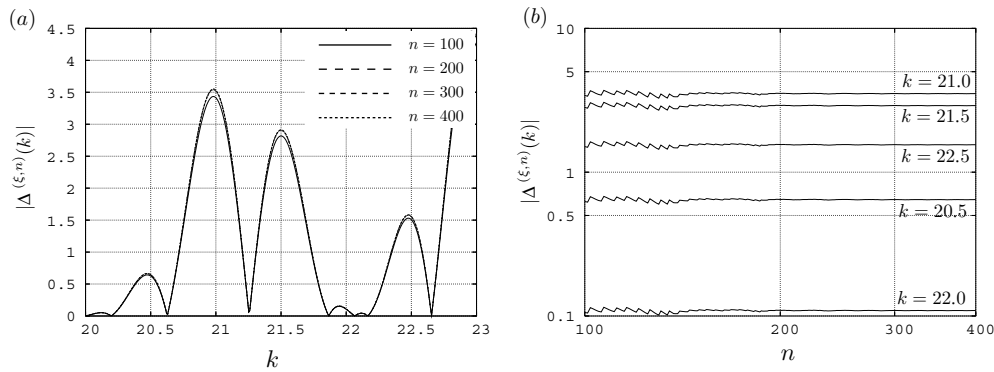


Figure 3. Plot of $\Delta^{(\xi,n)}(k)$ as a function of (a) k and (b) n . ξ is fixed at $|\partial\Omega|/200$.

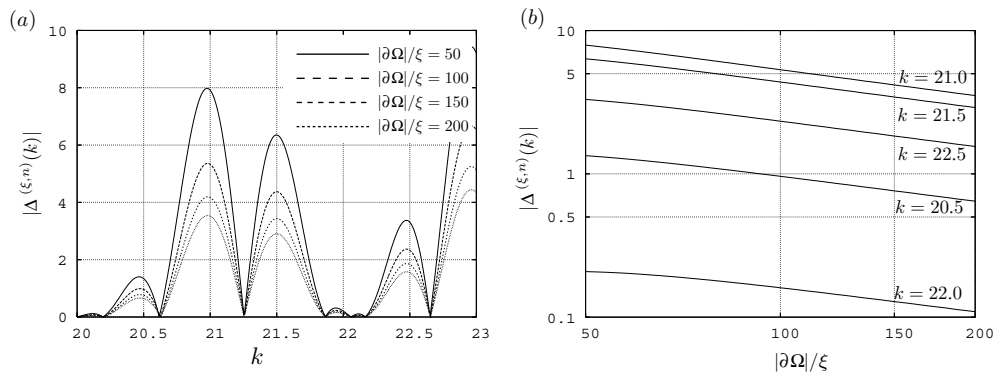


Figure 4. Plot of $\Delta^{(\xi,n)}(k)$ as a function of (a) k and (b) $|\partial\Omega|/\xi$. The number of quadrature points n is fixed at 400.

cutoff length $\xi \rightarrow 0$. In this plot, n is taken as 400, which ensures the convergence of $\Delta^{(\xi,n)}(k)$ from figure 3, meaning that in this ξ region $\Delta^{(\xi,n)}(k)$ can be regarded as $D^{(\xi)}(k)$. One further notes in figure 4(b) that the decay rate of $D^{(\xi)}(k)$ is algebraic and its exponents do not depend on k . This result strongly implies that even though $\lim_{n \rightarrow \infty} \Delta^{(n)}(k)$ may exist, it bears no meaningful information. Such behaviour of the determinant, as far as we have examined, is found for the domain with corners in general.

In the final part of this section, we show that $\Delta^{(n)}(k) \rightarrow 0$ is also observed in the standard calculation of the determinant $\Delta^{(n)}(k)$ if one discretizes it with some considerations for the quadrature points. Usually, the determinant (9) appearing in the standard BEM depends strongly on the configuration of quadrature points around the corners. It behaves wildly as a function of n , and it would be hard to find general trends. However, if we take, for example, the Gauss–Legendre quadrature rule to discretize the integral over each edge, we can verify that the determinant (9) vanishes in the same way as seen in figure 3. Figure 5 shows that the determinant (9) converges to zero. More importantly, one finds that the exponent of algebraic decrease looks uniform in k , namely

$$\lim_{n \rightarrow \infty} \Delta^{(n)}(k) \sim n^{-\alpha} \tilde{D}(k), \tag{20}$$

where α denotes a positive constant depending on the shape of the billiard table. This suggests the possibility that one can obtain the eigenvalues of equation (1) with (2) as zeros of $\tilde{D}(k)$

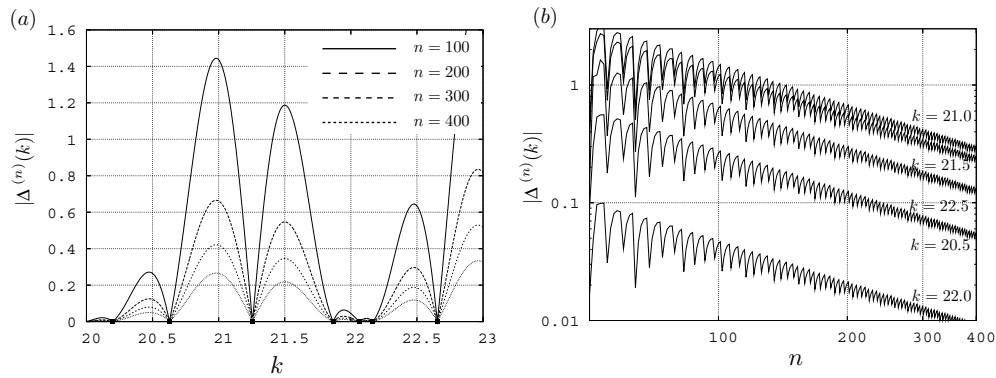


Figure 5. Plot of $\Delta^{(n)}(k)$, which appears in the standard BEM as a function of (a) k and (b) n . The squares on the k -axis represent analytically obtained eigenvalues.

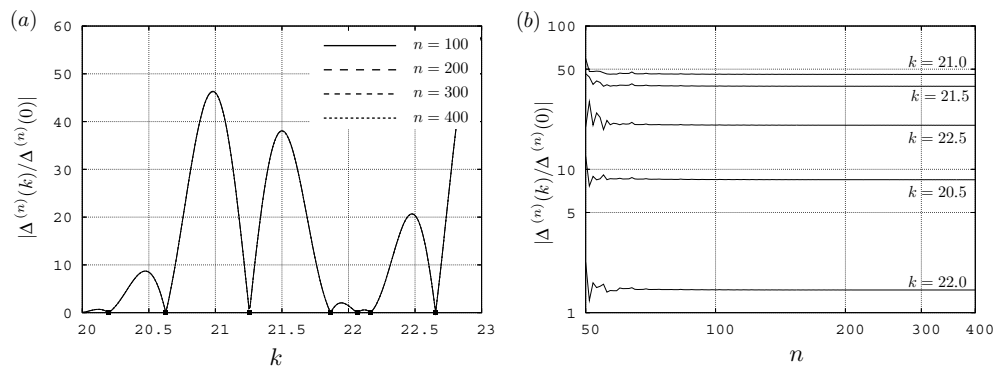


Figure 6. Plot of the ratio $\Delta^{(n)}(k)/\Delta^{(n)}(0)$ as a function of (a) k and (b) n . The squares on the k -axis represent analytically obtained eigenvalues.

even though the domain has corners. Figure 6 is a plot of the ratio $\lim_{n \rightarrow \infty} \Delta^{(n)}(k)/\Delta^{(n)}(0)$. As can also be seen, the zeros of $\tilde{D}(k)$ are in good agreement with correct eigenvalues. Such an idea was first proposed as an ‘*ad hoc* renormalization’ in [24].

In order to overcome these difficulties described above, we will reformulate a BEM derived from a non-singular integral equation. For the triangular domains, Pisani tackled the problem along this line, and successfully derived a non-singular integral equation based on the wedge Green’s function [24]. However, it is not so easy to generalize Pisani’s method to polygonal domains and more generally to domains with corners. It is also important to note that one cannot apply Pisani’s method to justify the standard BEM since the latter is based on the free Green’s function. In the next section, we consider an alternative non-singular integral equation based on the free Green’s function and give a modified BEM with a rigorous basis for domains with corners. A justification for ‘*ad hoc* renormalization’ is also given in the final part of the next section.

3. A BEM derived from non-singular integral equation

In this section, we will derive a non-singular integral equation from the original one (6). To this end, we apply the decomposition method [28]. If the operator

$$(\hat{K}\rho)(t) = \begin{cases} \int_{\partial\Omega} K(t, s; k)\rho(s) ds, & \mathbf{r}(t) \in \partial\Omega \setminus \{p_1, p_2, \dots, p_m\}, \\ \int_{\partial\Omega} K(t, s; k)\rho(s) ds + \left(1 - \frac{\gamma_i}{\pi}\right)\rho(t), & \mathbf{r}(t) \in \{p_1, p_2, \dots, p_m\}, \end{cases} \quad (21)$$

appearing in the integral equation (6) admits a decomposition $\hat{K} = \hat{K}_R + \hat{K}_S$ such that (i) \hat{K}_R is an integral operator whose kernel $K_R(t, s; k)$ is bounded and continuous on each $\partial\Omega \times \Gamma_i$, and (ii) \hat{K}_S is a bounded operator on $C^0(\partial\Omega)$ with $\|\hat{K}_S\| < 1$ for the maximum norm, then $(1 - \hat{K}_S)$ has a bounded inverse which is expressed as the Neumann series

$$(1 - \hat{K}_S)^{-1} = 1 + \hat{K}_S + \hat{K}_S^2 + \dots \quad (22)$$

As a result, the original integral equation $\rho - \hat{K}\rho = 0$ is converted into

$$\rho - (1 - \hat{K}_S)^{-1}\hat{K}_R\rho = 0. \quad (23)$$

Since the integral kernel

$$\tilde{K}(t, s; k) = [(1 - \hat{K}_S)^{-1}K_R(\cdot, s; k)](t) \quad (24)$$

is bounded and continuous on each $\partial\Omega \times \Gamma_i$, one can apply the Fredholm theory to solve the integral equation (23).

To obtain a required decomposition, consider the operator defined as

$$(\hat{K}_0\rho)(t) := \begin{cases} \int_{\partial\Omega} K_0(t, s)\rho(s) ds, & \mathbf{r}(t) \in \partial\Omega \setminus \{p_1, p_2, \dots, p_m\}, \\ \int_{\partial\Omega} K_0(t, s)\rho(s) ds + \left(1 - \frac{\gamma_i}{\pi}\right)\rho(t), & \mathbf{r}(t) = p_i \in \{p_1, p_2, \dots, p_m\}, \end{cases} \quad (25)$$

where $K_0(s, t)$ is a singular part of the kernel $K(t, s; k)$:

$$K_0(t, s) = -\frac{1}{\pi} \frac{[\mathbf{r}(s) - \mathbf{r}(t)] \cdot \mathbf{v}_s}{|\mathbf{r}(s) - \mathbf{r}(t)|^2}. \quad (26)$$

Note that $\hat{K}_0\rho$ belongs to $C^0(\partial\Omega)$ for arbitrary $\rho \in C^0(\partial\Omega)$. In fact, $-\hat{K}_0\rho$ is given as a sum of the interior and exterior boundary values Φ^\mp of the double-layer potential

$$\Phi(\mathbf{r}) = \int_{\partial\Omega} \frac{\partial H_0(\mathbf{r}, \mathbf{r}(s))}{\partial v_s} \rho(s) ds \quad (27)$$

with respect to a free Green's function of the Laplace equation

$$H_0(\mathbf{r}, \mathbf{r}') = -\frac{1}{2\pi} \ln \frac{1}{|\mathbf{r} - \mathbf{r}'|}, \quad (28)$$

because the following gap relation holds:

$$\Phi^\mp(\mathbf{r}(t)) = \begin{cases} \int_{\partial\Omega} \frac{\partial H_0(\mathbf{r}(t), \mathbf{r}(s))}{\partial v_s} \rho(s) ds \pm \frac{1}{2}\rho(t), & \mathbf{r}(t) \in \partial\Omega \setminus \Pi, \\ \int_{\partial\Omega} \frac{\partial H_0(\mathbf{r}(t), \mathbf{r}(s))}{\partial v_s} \rho(s) ds \pm \frac{\delta_i^\mp}{2}\rho(t), & \mathbf{r}(t) = p_i \in \{p_1, p_2, \dots, p_m\}, \end{cases} \quad (29)$$

where $\delta_i^- = \gamma_i/\pi$ and $\delta_i^+ = (2\pi - \gamma_i)/\pi$. Both the interior and exterior boundary values Φ^\mp are continuous, so $\hat{K}_0\rho$ is. However, the operator \hat{K}_0 is not suitable for our purpose, because $\|\hat{K}_0\rho\| = 1$ follows from the Green's theorem for the constant density $\rho(t) = 1$.

Therefore, we first introduce the cutoff operator $\hat{K}_S^{(\xi)}$ given as

$$(\hat{K}_S^{(\xi)} \rho)(t) := (\hat{K}_0 \rho)(t) - \int_{\partial\Omega} K_0(t, s) h_\xi(|t - s|) \rho(s) ds, \tag{30}$$

where h_ξ denotes the cutoff function defined as (18). Since, as shown above, $\hat{K}_0 \rho$ belongs to $C^0(\partial\Omega)$, $\hat{K}_S^{(\xi)} \rho$ also belongs to $C^0(\partial\Omega)$ for $\rho \in C^0(\partial\Omega)$. The norm of $\hat{K}_S^{(\xi)}$ is discussed later.

Second, we define $\hat{K}_R^{(\xi)}$ as

$$(\hat{K}_R^{(\xi)} \rho)(t) := \int_{\partial\Omega} K_R^{(\xi)}(t, s; k) \rho(s) ds, \quad r(t) \in \partial\Omega, \tag{31}$$

where

$$K_R^{(\xi)}(t, s; k) := K(t, s; k) - K_0(t, s)(1 - h_\xi(|t - s|)), \tag{32}$$

which is bounded and continuous on each $\partial\Omega \times \Gamma_i$. Combining (21), (30) and (31), we can see $\hat{K} = \hat{K}_S^{(\xi)} + \hat{K}_R^{(\xi)}$. Now, our remaining task to have a non-singular integral equation is just to check that the following inequality holds for a certain $\xi > 0$:

$$\|\hat{K}_S^{(\xi)} \rho\| < \|\rho\| \quad \text{for} \quad \rho \in C^0(\partial\Omega). \tag{33}$$

If the boundary consists of a single C^2 arc, one can always find a positive ξ such that the inequality (33) holds. In fact, for each boundary point $r(t) \in \partial\Omega$, we have

$$\begin{aligned} \left| \int_{\partial\Omega} K_S^{(\xi)}(t, s) \rho(s) ds \right| &\leq \left| \int_{t-\xi}^{t+\xi} K_0(t, s) \rho(s) ds \right| \\ &\leq 2\xi M \|\rho\|, \end{aligned} \tag{34}$$

since $K_0(s, t)$ can be continuously extended onto $\partial\Omega \times \partial\Omega$. Here M denotes an upper bound for $K_0(s, t)$. On the other hand, in the case of domains with corners, the inequality (33) is not trivial due to the divergence of the kernel $K_0(t, s)$. If neighbouring sides of corners are at most straight lines, the inequality

$$|\hat{K}_S^{(\xi)}| = \max_{i=1,2,\dots,m} \left| 1 - \frac{\gamma_i}{\pi} \right| < 1, \tag{35}$$

can be proved for sufficient small ξ [29]. More precisely, the case of the boundary value problem of the Laplace equation is discussed in [29], but one can directly adopt his proof into the present problem since the singular part of the integral kernel (7) is the same as that for the Laplace equation. Polygonal domains are typical examples of this class. In the appendix, we provide a proof of the inequality (33) for general domains with corners whose interior angles γ_i are positive. The technique used in the proof is essentially the same as that given in [29].

Now we formulate a well-grounded version of BEM by discretizing the integral equation

$$\rho(t) - \int_{\partial\Omega} \tilde{K}(t, s; k) \rho(s) ds = 0 \tag{36}$$

with the piecewise continuous kernel

$$\tilde{K}(t, s; k) = [(1 - \hat{K}_S^{(\xi)})^{-1} K_R^{(\xi)}(\cdot, s; k)](t). \tag{37}$$

To have a computable determinant, we consider an approximate integral kernel obtained by replacing the integrals in the definition of the kernel (37) with finite sums:

$$\begin{aligned} \tilde{K}^{(n')}(t, s; k) &= K_R^{(\xi)}(t, s; k) + \sum_{k_1=1}^{n'} m_{k_1} K_S^{(\xi)}(t, t_{k_1}) K_R^{(\xi)}(t_{k_1}, s; k) \\ &+ \sum_{k_1=1}^{n'} \sum_{k_2=1}^{n'} m_{k_1} m_{k_2} K_S^{(\xi)}(t, t_{k_2}) K_S^{(\xi)}(t_{k_2}, t_{k_1}) K_R^{(\xi)}(t_{k_1}, s; k) + \dots, \end{aligned} \tag{38}$$

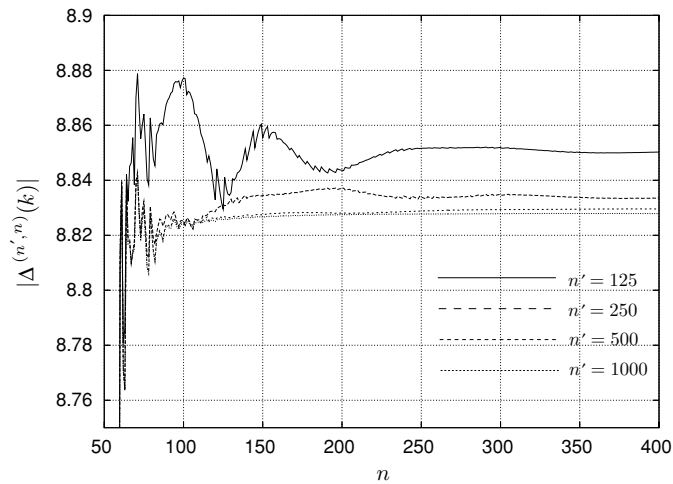


Figure 7. Plot of a novel determinant $\Delta^{(n',n)}(k)$ for $n' = 125, 250, 500, 1000$. k is set to 21.5.

and discretize the integral equation

$$\rho(t) - \int_{\partial\Omega} \tilde{K}^{(n')}(t, s; k) \rho(s) ds = 0 \quad (39)$$

to

$$\rho(s_i) - \sum_{j=1}^n w_j \tilde{K}^{(n')}(s_i, s_j; k) \rho(s_j) = 0. \quad (40)$$

Here $(\{t_1, t_2, \dots, t_{n'}\}, \{m_1, m_2, \dots, m_{n'}\})$ and $(\{s_1, s_2, \dots, s_n\}, \{w_1, w_2, \dots, w_n\})$ are independent quadrature rules. Since the Neumann series can be written in terms of the inverse matrix,

$$\delta_{kl} + m_l K_S^{(\xi)}(t_k, t_l) + \sum_{j_1=1}^{n'} m_{j_1} m_l K_S^{(\xi)}(t_k, t_{j_1}) K_S^{(\xi)}(t_{j_1}, t_l) + \dots = \{\delta_{kl} - K_S^{(\xi)}(t_k, t_l) m_l\}^{-1}, \quad (41)$$

we can reduce the $n \times n$ matrix $\tilde{K}^{(n')}(s_i, s_j; k)$ appearing in (40) to

$$\begin{aligned} \tilde{K}^{(n')}(s_i, s_j; k) &= K_R^{(\xi)}(s_i, s_j; k) + \sum_k^{n'} \sum_l^{n'} m_k K_S^{(\xi)}(s_i, t_k) \\ &\quad \times \{\delta_{kl} - K_S^{(\xi)}(t_k, t_l) m_l\}^{-1} K_R^{(\xi)}(t_l, s_j; k). \end{aligned} \quad (42)$$

Let us introduce a novel discretized determinant

$$\Delta^{(n',n)}(k) = \delta_{ij} - w_j K^{(n')}(s_i, s_j; k). \quad (43)$$

It is guaranteed by the Fredholm theory that $\Delta^{(n',n)}$ converges to the Fredholm determinant for (36), say $\tilde{D}^{(\xi)}(k)$, as $n \rightarrow \infty$ after taking $n' \rightarrow \infty$.

Figures 7 and 8 show the behaviour of $\Delta^{(n',n)}(k)$ for the $\pi/2$ – $\pi/3$ – $\pi/6$ -angled triangular domain. Here the cutoff length ξ is set to 0.25, which is a quarter of the length of the shortest edge of the triangle, and discretized boundary points and their weights are determined by the Gauss–Legendre quadrature rule. In figure 7, it can be confirmed that $\Delta^{(n',n)}(k)$ indeed

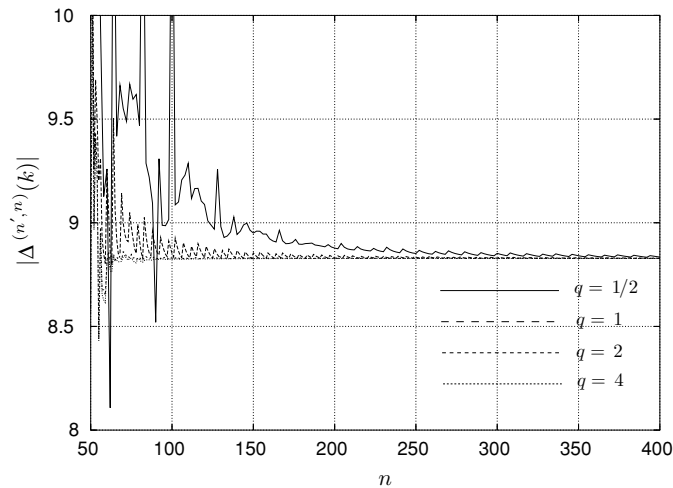


Figure 8. Plot of a novel determinant $\Delta^{(q n, n)}(k)$ for $q = 1/2, 1, 2, 4$. k is set to 21.5.

converges to a certain function of n as n' is increased, and $\lim_{n' \rightarrow \infty} \Delta^{(n', n)}(k)$ converges to a definite value with the increase of n . Figure 8 is a plot of $\Delta^{(n', n)}(k)$ for fixed several ratios $q = n'/n$. It can be found that the fluctuation of $\Delta^{(n', n)}(k)$ is less than 1% at $n = 60$, which is about four times as large as the number of quadrature points n_k estimated from the de Broglie wavelength, when $q = 4$.

One further notes in figure 8 that $\lim_{n \rightarrow \infty} \Delta^{(q n, n)}(k)$ does not depend on the choice of q . If this is the case for any region of k , it is possible to justify the ‘*ad hoc* renormalization’ method mentioned in the previous section. Taking $q = 1$, in fact, we can decompose the determinant $\Delta^{(n, n)}(k)$ into

$$\Delta^{(n, n)}(k) = \det[\delta_{ij} - K_S^{(\xi)}(s_i, s_j)w_j]^{-1} \det[\delta_{ij} - K(s_i, s_j; k)w_j], \quad (44)$$

where we take a common quadrature rule $(\{s_1, s_2, \dots, s_n\}, \{w_1, w_2, \dots, w_n\})$ to discretize the integral within the definition of the kernel (37) and that in the integral equation (36). Since the first term of the decomposition (44) is independent of k and the second one is exactly the determinant $\Delta^{(n)}(k)$ appearing in the standard BEM, the renormalized determinant should converge to the ratio of the well-defined Fredholm determinant of the integral equation (36):

$$\lim_{n \rightarrow \infty} \frac{\Delta^{(n)}(k)}{\Delta^{(n)}(0)} = \frac{\tilde{D}^{(\xi)}(k)}{\tilde{D}^{(\xi)}(0)}. \quad (45)$$

4. Summary and discussion

In this paper, we have reformulated the BEM for the domain with corners by deriving a non-singular integral equation. As mentioned in section 2, the standard BEM encounters a problem if the domain has corners. The problem is that the determinant appearing in the standard BEM vanishes everywhere due to the singularity of the integral kernel. We have solved such a difficulty by introducing a non-singular integral equation and presented a modified version of BEM based on it. It should be noted, however, that the present formulation cannot be applied to the domain with cusp-type corners, that is, the condition that $\gamma_i > 0$ should be satisfied, otherwise the singular part of the decomposed kernel is not normalizable.

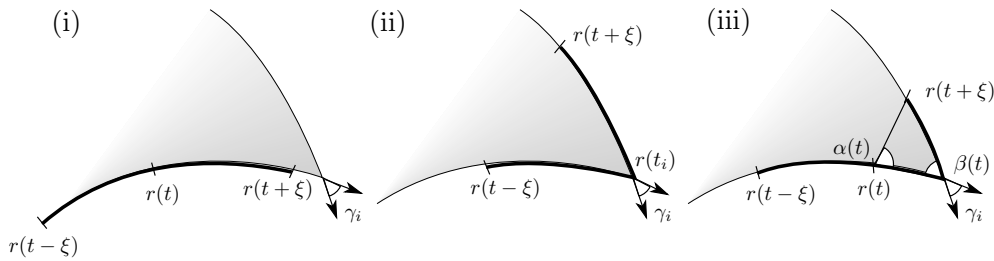


Figure 9. Boundary of the domain around a corner.

It might be of interest, as a next issue, to consider a semiclassical formula derived from the renormalized determinant. The Gutzwiller–Voros zeta function can be reformulated as a semiclassical limit of the determinant appearing in the standard BEM [30], and the semiclassical Fredholm determinant is also introduced based on the Fredholm theory [31]. Since most of the planar billiards whose classical ergodic aspects are well studied and for this reason often used for the test of semiclassical theories, have corners, semiclassical arguments based on the reformulated determinant may provide an alternative understanding of diffractive phenomena caused by singularities of the boundary. Especially in (42), we note that the integral kernel is given as a sum of the ‘long-range’ propagation and the convergent multiple scattering expansion of the ‘short-range’ correction. The former can naturally be approximated by the asymptotic form of the Hankel function in the semiclassical limit $k \rightarrow \infty$. On the other hand, the latter seems to require some other treatment even in the semiclassical regime. The relation between the Fredholm determinant and the diffractive corrections is to be investigated along this line.

Acknowledgment

The research at ATR was supported in part by the National Institute of Information and Communications Technology.

Appendix

In this appendix, we shall prove the key inequality (33). As mentioned in the text, we assume that a domain Ω is enclosed with the boundary $\partial\Omega$ consisting of a finite number of C^2 arcs $\{\Gamma_1, \Gamma_2, \dots, \Gamma_m\}$ and each corner has a positive interior angle γ_i . We take ξ small enough such that the interval $(\mathbf{r}(t - \xi), \mathbf{r}(t + \xi))$ along the boundary contains at most one corner and estimate $|\hat{K}_S^{(\xi)}\rho(t)|$ in the following three cases.

(i) The interval $(\mathbf{r}(t - \xi), \mathbf{r}(t + \xi))$ is contained in a single arc (see figure 9(i)): in this case, we have

$$\left| \int_{\partial\Omega} K_S^{(\xi)}(t, s)\rho(s) ds \right| \leq 2\xi M \|\rho\|, \quad (\text{A.1})$$

because each restriction of $K_0(t, s)$ to $\Gamma_i \times \Gamma_i$ is bounded. Here

$$M = \max_{i=1,2,\dots,m} \sup_{t,s \in \Gamma_i} |K_S(t, s)|. \quad (\text{A.2})$$

(ii) The interval $(\mathbf{r}(t - \xi), \mathbf{r}(t + \xi))$ contains a corner and $t \neq t_i$ (see figure 9(ii)): in this case, without loss of generality, we can assume that $\mathbf{r}(t - \xi)$ and $\mathbf{r}(t)$ are contained in Γ_i and

$\mathbf{r}(t + \xi)$ in Γ_{i+1} as illustrated in figure 9(ii). Then, we estimate the integral as

$$\begin{aligned} \left| \int_{\partial\Omega} K_S^{(\xi)}(t, s)\rho(s) \, ds \right| &\leq \left| \int_{t-\xi}^{t+\xi} K_0(t, s)\rho(s) \, ds \right| \\ &\leq \left| \int_{t-\xi}^{t_i} K_0(t, s)\rho(s) \, ds \right| + \left| \int_{t_i}^{t+\xi} K_0(t, s)\rho(s) \, ds \right|, \end{aligned} \tag{A.3}$$

in which the first term is bounded by $2\xi M \|\rho\|$. Since the second term can be evaluated as

$$\begin{aligned} \left| \int_{t_i}^{t+\xi} K_0(t, s)\rho(s) \, ds \right| &\leq \|\rho\| \int_{t_i}^{t+\xi} |K_0(t, s)| \, ds \\ &= \|\rho\| \cdot \left| \int_{t_i}^{t+\xi} K_0(t, s) \, ds \right| \\ &= \|\rho\| \cdot \left| \frac{\alpha(t)}{\pi} \right|, \end{aligned} \tag{A.4}$$

where $\alpha(t)$ denotes the angle $\angle \mathbf{r}(t + \xi)\mathbf{r}(t)\mathbf{r}(t_i)$. Here, in addition to the above requirement, we have chosen ξ such that the sign of $K_0(t, s)$ is constant for $t \in (t_i - \xi, t_i)$ and $s \in (t_i, t_i + \xi)$, where $\mathbf{r}(t_i) = p_i$ for $i = 1, 2, \dots, m$. Due to our assumption for the geometry of domains, such a choice is always possible. Thus, we have

$$\left| \int_{\partial\Omega} K_S^{(\xi)}(t, s)\rho(s) \, ds \right| \leq \|\rho\| \left(2\xi M + \left| \frac{\alpha(t)}{\pi} \right| \right). \tag{A.5}$$

Here we note

$$\alpha(t) = |\pi - \beta(t)|, \tag{A.6}$$

where $\beta(t) = \angle \mathbf{r}(t)\mathbf{r}(t_i)\mathbf{r}(t + \xi)$, and $\beta(t) = \gamma_i + \mathcal{O}(\xi)$ for small ξ since each boundary arc is assumed to be C^2 .

(iii) $t = t_i$ (see figure 9(iii)): in this case, we have

$$\begin{aligned} |(\hat{K}_S^{(\xi)}\rho)(t_i)| &\leq \|\rho\| \left(\int_{t_i-\xi}^{t_i} |K_0(t_i, s)| \, ds + \int_{t_i}^{t_i+\xi} |K_0(t_i, s)| \, ds \right) + \left| 1 - \frac{\gamma_i}{\pi} \right| \cdot |\rho(t_i)| \\ &\leq \|\rho\| \left(2\xi M + \left| 1 - \frac{\gamma_i}{\pi} \right| \right). \end{aligned} \tag{A.7}$$

Here ξ should satisfy the same condition as in (ii). Taking account of (A.1), (A.5) and (A.7), we can finally confirm that there exists $\xi > 0$ which satisfies $\|\hat{K}_S^{(\xi)}\rho\| < \|\rho\|$.

References

- [1] Gutzwiller M C 1990 *Chaos in Classical and Quantum Mechanics* (New York: Springer)
- [2] Bohigas O 1991 *Les Houches Summer School Session LII* ed M J Giannoni, A Voros and J Zinn-Justin (Amsterdam: North-Holland) pp 87–199
- [3] Shudo A and Shimizu A 1993 *Phys. Rev. E* **47** 54–62
- [4] Bogomonly E, Giraud O and Schmit C 2001 *Commun. Math. Phys.* **222** 327–69
- [5] Vattay G, Wirzba A and Rosenqvist P E 1994 *Phys. Rev. Lett.* **73** 2304–07
- [6] Pavloff N and Schmit C 1995 *Phys. Rev. Lett.* **75** 61–4
- [7] Whelan N D 1995 *Phys. Rev. E* **51** 3778–81
- [8] Kac M 1966 *Am. Math. Mon.* **73** 1–23
- [9] Gordon C, Webb D and Wolpert S 1992 *Invent. Math.* **110** 1–22
- [10] Buser P, Conway J, Doyle P and Semmler K D 1994 *Int. Math. Res. Not.* **9** 391–400
- [11] Okada Y and Shudo A 2001 *J. Phys. A: Math. Gen.* **34** 5911–22
- [12] Giraud O 2004 *J. Phys. A: Math. Gen.* **37** 2751–64

-
- [13] Okada Y, Shudo A, Harayama T and Tasaki S 2005 *J. Phys. A: Math. Gen.* **38** L163–70
 - [14] Heller E J 1991 *Les Houches Summer School Session LII* ed M J Giannoni, A Voros and J Zinn-Justin (Amsterdam: North-Holland) pp 547–663
 - [15] Gutkin B 2003 *J. Phys. A: Math. Gen.* **36** 8603–22
 - [16] Vega J L, Uzer T and Ford J 1995 *Phys. Rev. E* **52** 1490–96
 - [17] Berry M V 1994 *J. Phys. A: Math. Gen.* **27** L391–8
 - [18] Cohen D, Lepore N and Heller E J 2001 *Preprint nlin.CD/0108014*
 - [19] Berry M V and Wilkinson M 1984 *Proc. R. Soc. Lond.* **392** 15–43
 - [20] Riddell R J 1979 *J. Comput. Phys.* **31** 21–41
Riddell R J 1979 *J. Comput. Phys.* **31** 42–59
 - [21] Boasman P A 1994 *Nonlinearity* **7** 485–537
 - [22] Bäcker A 2002 *Preprint nlin.CD/0204061*
 - [23] Hornberger K and Sminalsky U 2000 *J. Phys. A: Math. Gen.* **33** 2829–55
 - [24] Pisani C 1996 *Ann. Phys.* **251** 208–65
 - [25] Georgeot B and Prange R E 1995 *Phys. Rev. Lett.* **74** 2851–54
 - [26] Tasaki S, Harayama T and Shudo A 1997 *Phys. Rev. E* **56** R13–6
 - [27] Mizohata S 1958 *The Theory of Partial Differential Equations* (Cambridge: Cambridge University Press)
 - [28] Courant D and Hilbert D 1989 *Methods of Mathematical Physics* (New York: Wiley)
 - [29] Kress R 1999 *Linear Integral Equations* 2nd edn (Berlin: Springer)
 - [30] Harayama T and Shudo A 1992 *Phys. Lett. A* **165** 417–26
 - [31] Harayama T, Shudo A and Tasaki S 1999 *Nonlinearity* **12** 1113–49